# A General Method for Small Signal Stability Analysis

Yuri V. Makarov Zhao Yang Dong David J. Hill

Department of Electrical Engineering
The University of Sydney
NSW 2006, Australia

*Abstract*— **This paper presents a new general method for computing the different specific power system small signal stability conditions. The conditions include the points of minimum and maximum damping of oscillations, saddle node and Hopf bifurcations, and load flow feasibility boundaries. All these characteristic points are located by optimizing an eigenvalue objective function along the rays specified in the space of system parameters. The set of constraints consists of the load flow equations, and requirements applied to the dynamic state matrix eigenvalues and eigenvectors. Solutions of the optimization problem correspond to specific points of interest mentioned above. So, the proposed general method gives a comprehensive characterization of the power system small signal stability properties. The specific point obtained depends upon the initial guess of variables and numerical methods used to solve the constrained optimization problem. The technique is tested by analyzing the small signal stability properties for well-known example systems.**

## I. Introduction

Modern power grids are becoming more and more stressed with the load demands increasing rapidly. The voltage collapses which occurred recently have again drawn much attention to the issue of stability security margins in power systems [1]. The small signal stability margins are highly dependent upon such system factors as load flow feasibility boundaries, minimum and maximum damping conditions, saddle node and Hopf bifurcations, etc. Unfortunately, it is very difficult to say in advance which of these factors will make a decisive contribution to instability. Despite the progress achieved recently, the existing approaches deal with these factors independently - see [2], [3] for example, and additional attempts are needed to get a more comprehensive view on small-signal stability problem.

To study the power system small signal stability problem, an appropriate model for the machine and load dynamics is required. For example, the models given in [4] - [11] can be used. They include generator and excitation system differential equations, stator and network algebraic equations. These equations build up the set of differential-algebraic equations (1)

$$\begin{aligned} \dot{x_1} &= F(x_1, x_2, y, \tau) \\ 0 &= G(x_1, x_2, y, \tau) \end{aligned} \tag{1}$$

In the equation (1), $x_1$ is the vector of state (differential) variables, $x_2$ is the vector of algebraic variables, $y$ is the vector of specified system parameters, and $\tau$ is a parameter chosen for bifurcation analysis. In many cases $y$ is a function of $\tau$.

In the small signal stability analysis, the set (1) is then linearized at an equilibrium point to get the system Jacobian and state matrix. The structure of the system Jacobian $J$ is shown in Fig. 1 (which follows the structure given in [12]), where $J_{lf}$ stands for the load flow Jacobian, $J_{11} = \partial F/\partial x_1$, $J_{12} = \partial F/\partial x_2$, $J_{21} = \partial G/\partial x_1$ and $J_{22} = \partial G/\partial x_2$ are different parts of J corresponding to differential and algebraic variables. In Fig. 1, $Q_{gen}$ stands for the reactive power at generator buses, $P_{sb}$ is the active power at the swing bus, $\delta$ is the vector of machine rotor angles, $\omega$ is the vector of machine speeds, $\kappa$ is the vector of the state variables except $\delta$ and $\omega$ (such as $E'_q$, $E'_d$, $E_{fd}$, $V_R$, and $R_F$; load bus voltages $V_{load}$ and angles $\theta_{load}$ should be considered as dynamic state variables in cases where load dynamics is considered [12]), $i_d$ and $i_q$ are vectors of d-axis and q-axis currents; $V_{gen}$ and $V_{load}$ stand for generator and load bus voltages; $\theta_{sb}$ is the swing bus voltage angle, and $\theta$ denotes voltage angles at all buses except the swing bus. The prefix $\Delta$ means a small increment in corresponding variables.

The problem addressed here is that these different small signal stability conditions correspond to different physical phenomena and mathematical descriptions [13]. Saddle node bifurcations happen where the state matrix

$$\tilde{J} = J_{11} - J_{12}J_{22}^{-1}J_{21}$$

becomes singular and, for example, a static (aperiodic) type of voltage collapse or angle instability may be observed as a result. Hopf bifurcations occur when the system state matrix $\tilde{J}$ has a pair of conjugate eigenvalues passing the imaginary axis while the other eigenvalues have negative real parts, and the unstable oscillatory behavior may be seen. Singularity induced bifurcations are caused by singularity of the algebraic submatrix $J_{22}$ - see Fig. 1, and

PE-153-PWRS-16-09-1997 A paper recommended and approved by the IEEE Power System Engineering Committee of the IEEE Power Engineering Society for publication in the IEEE Transactions on Power Systems. Manuscript submitted May 27, 1997; made available for printing September 30, 1997.

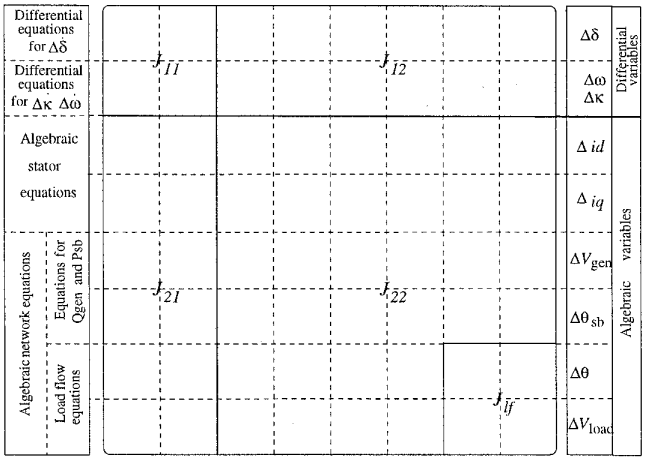


Fig. 1. Structure of the system Jacobian.

they result in fast collapse type of instability [14]. The load flow feasibility boundary corresponds to a surface where the load flow Jacobian matrix $J_{lf}$ is singular, and it restricts a region in the space of power system parameters where load flow solutions exist. Under certain modeling simplifications, this boundary coincides with the saddle node bifurcation conditions [15], [16], but in general case it should be taken into account separately.

To locate the saddle node and Hopf bifurcations along a given ray in the space of $y$, the following equation can be employed [2], [3], [17], [18]:

$$f(x, y_0 + \tau\Delta y) = 0 \quad (2)$$
$$\tilde{J}^t(x, y_0 + \tau\Delta y)l' + \omega l'' = 0 \quad (3)$$
$$\tilde{J}^t(x, y_0 + \tau\Delta y)l'' - \omega l' = 0 \quad (4)$$
$$l'_i - 1 = 0 \quad (5)$$
$$l''_i = 0 \quad (6)$$

where $\omega$ is the imaginary part of a system eigenvalue; $l'$ and $l''$ are real and imaginary parts of the corresponding left eigenvector $l$; $l'_i + jl''_i$ is the $i-th$ element of the left eigenvector $l$; $y_0 + \tau\Delta y$ specifies a ray in the space of $y$; $\tilde{J}$ stands for the state matrix obtained from the linearized model given in Fig. 1 provided that the algebraic submatrix $J_{22}$ is nonsingular.

In the above set, (2) is the load flow equation and conditions (3)-(6) provide an eigenvalue with zero real part and the corresponding left eigenvector.

Solutions of the system (2)-(6) correspond to either saddle node ($\omega = 0$) or Hopf ($\omega \neq 0$) bifurcations. Nevertheless the extreme load flow feasibility conditions (if they do not coincide with the saddle node bifurcations) can not be located by means of this system. Actually, if the load flow feasibility boundary is met on the ray $y_0 + \tau\Delta y$ but there is no an eigenvalue with zero real part, the system (2)-(6) becomes inconsistent and has no a solution.

Therefore, if the system (2)-(6) is used, it is necessary to analyze the load flow feasibility conditions additionally. The corresponding procedures are well known - see [2], [19], [20] for instance. The general idea behind these procedures

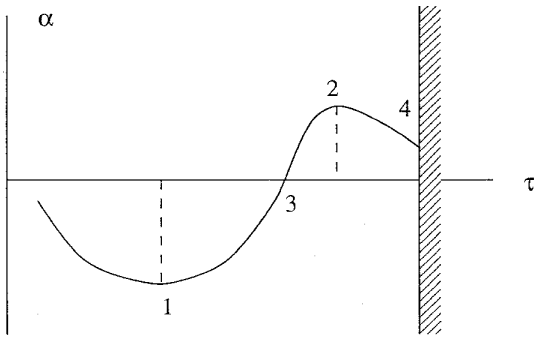


Fig. 2. Different solutions of the problem (10)-(15):
1,2 - minimum and maximum damping
3 - saddle ($\omega = 0$) or Hopf ($\omega \neq 0$) bifurcations
4 - load flow feasibility boundary

is illustrated by the following system:

$$f(x, y_0 + \tau\Delta y) = 0 \quad (7)$$
$$J^t_{lf}(x, y_0 + \tau\Delta y)l = 0 \quad (8)$$
$$l_i - 1 = 0 \quad (9)$$

where $l$ is the left eigenvector corresponding to a zero eigenvalue of the load flow Jacobian matrix $J_{lf}$. The system (7)-(9) gives the load flow feasibility boundary points along the ray $y_0 + \tau\Delta y$ by a similar way as the system (2)-(6) generates saddle node and Hopf bifurcation points.

By subsequent solution of both the problems (2)-(6) and (7)-(9) the general issue may be resolved, but a challenging task is to find a procedure which can generate all small-signal characteristic points by itself.

## II. General method

To locate the saddle node and Hopf bifurcations as well as the load flow feasibility boundary points within one procedure, the following constraint optimization problem is proposed

$$\alpha^2 \Rightarrow max/min \quad (10)$$

subject to

$$f(x, y_0 + \tau\Delta y) = 0 \quad (11)$$
$$\tilde{J}^t(x, y_0 + \tau\Delta y)l' - \alpha l' + \omega l'' = 0 \quad (12)$$
$$\tilde{J}^t(x, y_0 + \tau\Delta y)l'' - \alpha l'' - \omega l' = 0 \quad (13)$$
$$l'_i - 1 = 0 \quad (14)$$
$$l''_i = 0 \quad (15)$$

where $\alpha$ is the real part of an eigenvalue of interest.

The problem may have a number of solutions, and all of them presents different aspects of the small-signal stability problem as shown in Fig. 2.

The minimum and maximum damping points 1 and 2 correspond to zero derivative $d\alpha/d\tau$. The constraint set (11)-(15) gives all unknown variables at these points. The minimum and maximum damping, determined for all oscillatory modes of interest, provides an essential information about damping variations caused by a directed change of power system parameters.

The saddle node or Hopf bifurcations 3 correspond to $\alpha = 0$. They indicate the small-signal stability limits along the specified loading trajectory $y_0 + \tau\Delta y$. Besides revealing the type of instability (aperiodic for $\omega = 0$ or oscillatory for $\omega \neq 0$), the constraint set (11)-(15) gives the frequency of critical oscillatory mode. The left eigenvector $l = l' + jl''$ (together with the right eigenvector $r = r' + jr''$ which can be easily computed in its turn) determine such essential factors as sensitivity of $\alpha$ with respect to $y$, the mode, shape, participation factors, observability and excitability of the critical oscillatory mode [21] –[23].

The load flow feasibility boundary points 4 reflect the maximal power transfer capabilities of the power system. Those conditions play a decisive role when the system is stable everywhere on the ray $y_0 + \tau\Delta y$ up to the load flow feasibility boundary. The optimization procedure stops at these points as the constraint (11) can not be satisfied anymore.

A strict proof of the optimality conditions in the load flow feasibility points requires a complicated mathematical analysis, and we will not give this proof in the paper. Some initial ideas of this proof are briefly reported in the sequel.

Consider the trajectory of $x(\tau)$, $\tau \to \infty$ satisfying (11). At the load flow feasibility point, parameter $\tau$ can not be increased anymore beyond its limit value $\tau_*$. Nevertheless, the trajectory $x(\tau)$ can be smoothly continued by further decreasing $\tau$ see [24], for example. Suppose that the function $\alpha[x(\tau)]$ is monotonous and continuous in vicinity of $\tau_*$, say, along the trajectory $x(\tau)$, the increment $d\alpha$ is positive. As the increment $d\tau$ changes its sign at the point $\tau_*$, this means that the derivative $d\alpha/d\tau$ changes its sign at $\tau_*$. Thus the enough optimality conditions (the constant sign of the second derivative of the objective function with respect to $\tau$) are met at the point $\tau_*$ [33].

The problem (10)-(15) takes into account only one eigenvalue each time. The procedure must be repeated for all eigenvalues of interest. The choice of eigenvalues depends upon the concrete task to be solved. The eigenvalue sensitivity, observability , excitability and controllability factors [21], [22] can help to determine the eigenvalues of interest, and trace them during optimization. For example, the interarea oscillatory modes can be identified and then analyzed using (10)-(15).

The result of optimization depends on the initial guesses for all variables in (10)-(15). To get all characteristic points for a selected eigenvalue, different initial points may be computed for different values of $\tau$. At each point, the load flow conditions, state matrix eigenvalues and eigenvectors can be obtained, and then a particular eigenvalue selected to start the optimization procedure. More effective approaches for finding all characteristic points require additional development. At the moment we are analyzing the possibility to use the Genetic Algorithms for this purpose.

## III. Testing and validation of the method

Our purpose here is to demonstrate whether the proposed method is able to locate all these characteristic points depending on the initial guesses of $\tau$, $x$, $\alpha$, $\omega$, $l'$ and $l''$. The results will be then validated by comparing some of them with the results obtained in other papers, and by transient simulations conducted at the characteristic points.

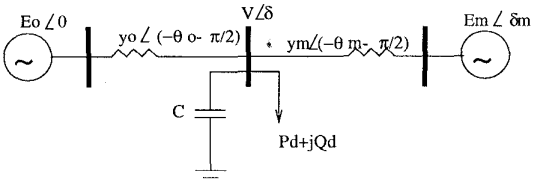


Fig. 3. The single-machine infinite-bus power system model

The single machine infinite bus power system model [25] presented in Fig. 3, and 3 machine 9 bus power system [26] shown in Fig. 12 will be studied here. Similar models were studied in [4] -[6], [17], [26] –[30].

The standard Gauss -Newton procedure from *Matlab* was used here for optimization [31].

### A. Single Machine Infinite Bus Power System Model

The model consists of four differential equations, which cover both generator and load dynamics [25].

The mathematical model of the system is the following:

$$\dot{\delta_m} = \omega \tag{16}$$

$$M\dot{\omega} = -d_m\omega + P_m + \\ +E_m y_m V sin(\delta - \delta_m - \theta_m) + \\ +E_m^2 y_m sin\theta_m \tag{17}$$

$$K_{qw}\dot{\delta} = -K_{qv2}^2 V^2 - K_q v V + \\ +E_0' y_0' V cos(\delta + \theta_0') + \\ +E_m y_m V cos(\delta - \delta_m + \theta_m) - \\ -(y_0' cos\theta_0 + y_m cos\theta_m)V^2 - \\ -Q_0 - Q_1 \tag{18}$$

$$k_4\dot{V} = K_{pw}K_{qv}^2 V^2 + (K_{pw}K_{qv} - K_{qw}K_{pv})V + \\ +\sqrt{K_{qw}^2 + K_{pw}^2}[-E_0' y_0' V cos(\delta + \theta_0 - h) - \\ -E_m y_m V cos(\delta - \delta_m + \theta_m - h) + \\ +(y_0' cos(\theta_0 - h) + y_m cos(\theta_m - h))V^2] - \\ -K_{qw}(P_0 + P_1) + K_{pw}(Q_0 + Q_1) \tag{19}$$

where $k_4 = TK_{qw}K_{pv}$ and $h = tan^{-1}(K_{qw}/K_{pw})$. Parameters of the system are the following [25]: $K_{pw} = 0.4$, $K_{pv} = 0.3$, $K_{qw} = -0.03$, $K_{qv} = -2.8$, $K_{qv2} = 2.1$, $T = 8.5$, $P_0 = 0.6$, $Q_0 = 1.3$; $P_1$ and $Q_1$ are taken zero at the initial operating point.

Network and generator values are: $y_0 = 20.0$, $q_0 = -5.0$, $E_0 = 1.0$, $C = 12.0$, $y_0' = 8.0$, $\theta_0' = -12.0$, $E_0' = 2.5$, $y_m = 5.0$, $\theta_m = -5.0$, $E_m = 1.0$, $P_m = 1.0$, $M = 0.3$, $\delta_m = 0.05$.

All parameters are given in per unit except for angles, which are in degrees. The active and reactive loads are featured by the following equations:

$$P_d = P_0 + P_1 + K_{pw}\delta + K_{pv}(V + T\dot{V}) \tag{20}$$

$$Q_d = Q_0 + Q_1 + K_{qw}\delta + K_{qv}V + K_{qv2}V^2 \tag{21}$$

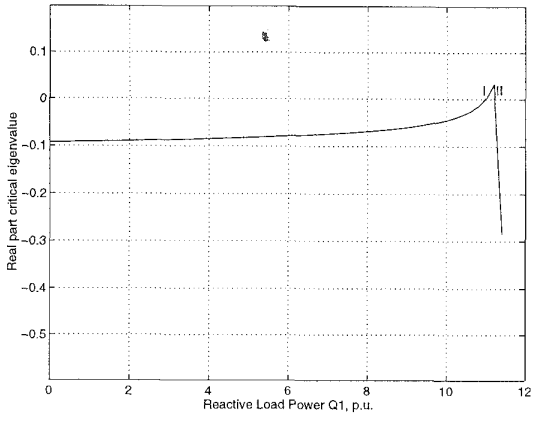


Fig. 4. $\alpha = Re\lambda$ computed for $P_1 = 0$ and $Q_1$ =variable

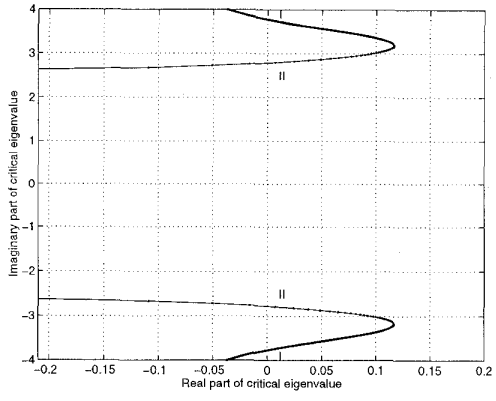


Fig. 5. Subcritical (I) and supercritical (II) bifurcations

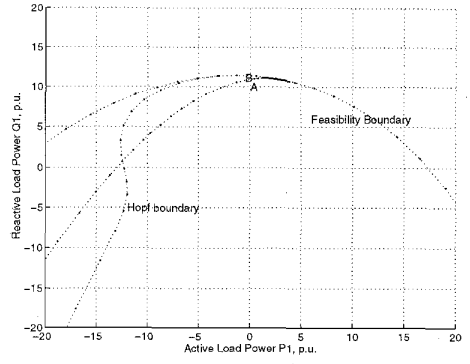


Fig. 6. The feasibility and Hopf bifurcation boundaries

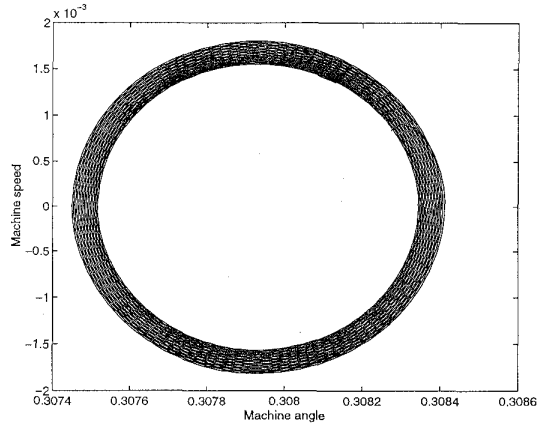


Fig. 7. Phase portrait at point A near subcritical bifurcation

The system (16)-(19) depends on four state variables $\delta$, $\delta_m$, $\omega$, $V$. Their values at the initial load flow point are the following: $\delta = 2.75$, $\delta_m = 11.37$, $\omega = 0$, and $V = 1.79$. Note that the initial point is not a physical solution as the voltage $V$ is too high as $Q_1$ is zero.

The results of numerical simulations are presented in in Fig. 4-11.

The dependence of the real part $\alpha = Re\lambda$ of critical eigenvalue $\lambda$ upon $Q_1$ is shown in Fig. 4. It is seen that there are both subcritical (point I) and supercritical (point II) Hopf bifurcations along the chosen loading direction. Fig. 5 presents the root locus for the critical eigenvalue conjugate. The subcritical (point I) and supercritical (point II) Hopf bifurcation points are displayed. Both these characteristic points were successfully located by the proposed method, (10 -15).

Fig. 6. shows the load flow feasibility and bifurcation boundaries on the plane of the load parameters $P_1$ and $Q_1$. The boundaries were obtained by the proposed optimization method when the loading direction was changed by subsequent rotation of $\Delta y$ in the plane $P_1$ and $Q_1$. Exactly the same curves were computed in [17] by separate solution of the problems (2)-(6) and (7)-(9). To verify the results, transient simulations were performed at several points in the plane $P_1$ - $Q_1$. Point A with $P_1 = 0$ and $Q_1 = 10.88$ was placed within the load flow feasibility region close to subcritical bifurcation boundary. Then a small disturbance was applied. The corresponding phase portrait is shown in Fig. 7. In a complete correspondence with the theoretical expectations, the system has experienced sustained oscillations.

Those oscillations can be viewed in Fig. 8 where the load bus voltage against time is presented.

Point B with $P_1 = 0$ and $Q_1 = 11.4$ was placed within the load flow feasibility region close to the supercritical bifurcation boundary. (Note that, in the vicinity of points A and B, the Hopf bifurcation boundary as shown in Fig. 6 actually consists of internal subcritical and external supercritical boundaries located very closely). All eigenvalues at point B have small negative real parts. The phase portrait for a small disturbance applied at point B is given in Fig. 9. The system undergoes decreasing oscillations. The corresponding voltage behavior is shown in Fig. 10.

The next point was taken close to the point B but outside the load flow feasibility boundary. The system experiences voltage collapse as illustrated by Fig. 11.

By solving the optimization problem, the system small signal stability boundaries were obtained.

The minimum and maximum damping conditions on the plane $P_1$ - $Q_1$ were studied as well. Table 1 presents the

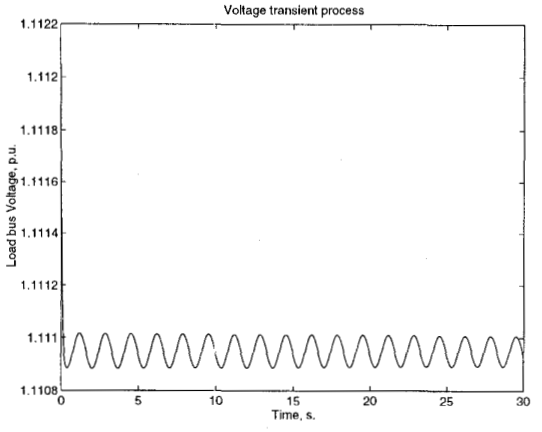


Fig. 8. Transient process near subcritical bifurcation (point A)

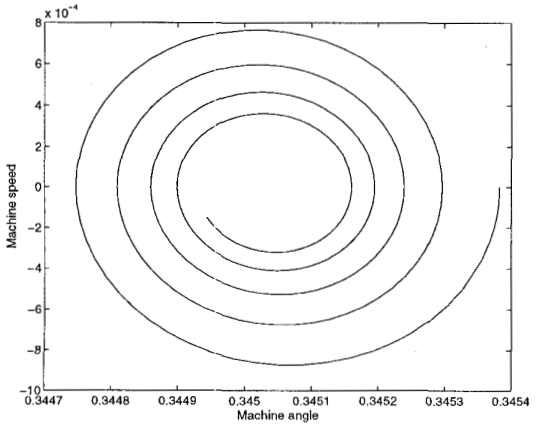


Fig. 9. Phase portrait at point B near supercritical bifurcation

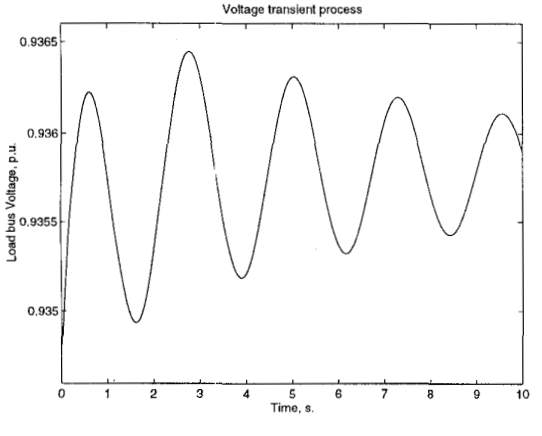


Fig. 10. Load bus voltage transients near supercritical bifurcation

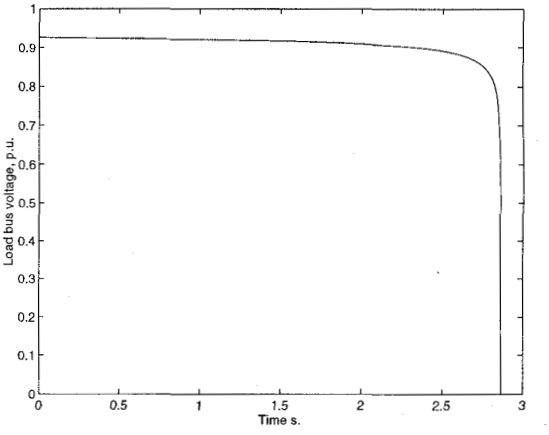


Fig. 11. The system load bus voltage transients near feasibility boundary

TABLE 1
MINIMUM AND MAXIMUM DAMPING CURVES FOR THE SINGLE-MACHINE INFINITE-BUS SYSTEM

| min-damping | | max-damping | |
|---|---|---|---|
| $P_1$ | $Q_1$ | $P_1$ | $Q_1$ |
| -2.5709 | -7.9124 | -4.5537 | -0.9679 |
| -0.8391 | -3.1315 | -4.6069 | -1.2344 |
| 0.0111 | 0.2113 | -4.7900 | -2.1326 |
| 0.0000 | 0.3836 | -4.9317 | -2.8473 |
| -0.0165 | 0.3152 | -5.0219 | -3.2612 |
| -0.107 | 1.0240 | -5.1184 | -3.7187 |
| -0.1131 | 0.7142 | -5.2218 | -4.2286 |
| -0.1640 | 0.7717 | -5.3329 | -4.8017 |

curves of minimum and maximum damping for different eigenvalues.

### *B. Three-Machine Nine-Bus Power System Model*

The power system model is composed of 3 machines and 9 buses [26] as shown in Fig. 12. Stability studies for a similar system can be found in [4], [30]. The machines of the system are modeled by using the classical model for machine 1 and two-axis model for machines 2 and 3 - see equations (22) –(27).

$$\tau_{j1}\dot{\omega}_1 = T_{m1} - E_1 I_{q1} - D_1\omega_1 \quad (22)$$

$$\dot{\delta}_1 = \omega_1 \quad (23)$$

$$\tau'_{q0i}\dot{E}'_{di} = -E'_{di} - (x_{qi} - x'_i)I_{qi} \quad (24)$$

$$\tau'_{d0i}\dot{E}'_{qi} = E_{FDi} - E'_{qi} + (x_{di} - x'_i)I_{di} \quad (25)$$

$$\tau_{ji}\dot{\omega}_i = T_{mi} - D_i\omega_i - I_{di0}E'_{di} - I_{qi0}E'_{qi} - E'_{di0}I_{di} - E'_{qi0}I_{qi} \quad (26)$$

$$\dot{\delta}_i = \omega_i \quad (27)$$

$$i = 2, 3$$

Unlike [4] and [30], in our tests we neglected the excitation system dynamics, so our state variables were the following: $\delta$, $\omega$, $E'_q$, and $E'_d$. Algebraic variables were $I_d$, $I_q$, $\theta$, and $V$; bifurcation parameters were $P_{ld}$ and $Q_{ld}$. . The notations, parameter values and description of the system (22) –(27) can be found in [26].

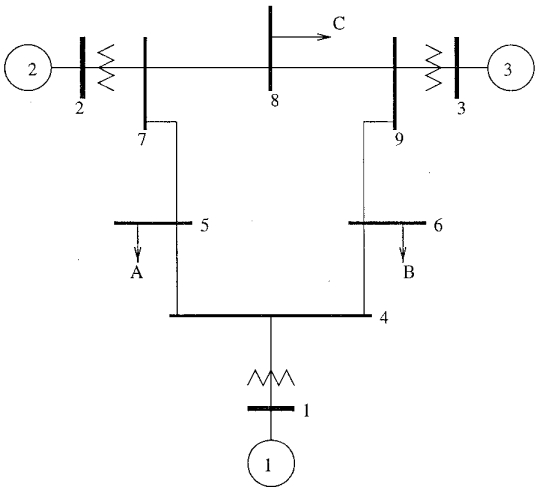


Fig. 12. The 3-machine 9-bus system

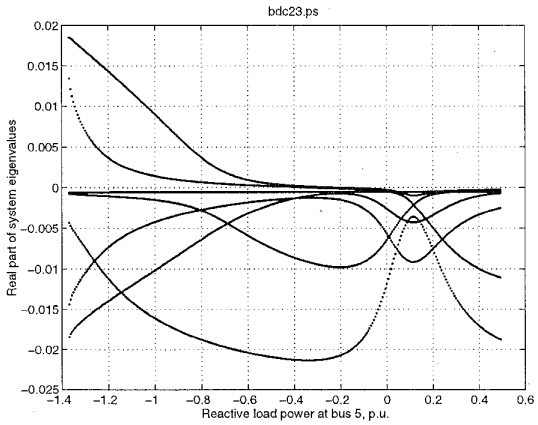


Fig. 13. Real parts of system eigenvalues vs reactive power

Unlike the used single machine infinite bus model, which includes an induction motor load, this 3 machine 9 bus model considers constant load models only. In the general case of small signal stability analysis, the load dynamics should be definitely taken into consideration, but nevertheless some stability aspects can be studied with the constant load model [32].

In the preliminary examination, the loads $P_{ld}$ and $Q_{ld}$ at buses 5, 6 and 8 were increased in proportion with the load size. The increase of load was followed by the corresponding increase of generation in proportion with the generator size. The total increment in load was equal to the total increment in generation. The loading was repeated till the point where load flow did not converge. At each step, eigenvalues of the state matrix were computed to reveal the bifurcation points and minimum and maximum damping conditions.

The system eigenvalue behavior along the chosen loading direction is shown in Fig. 13.

There are several points of interest which can be clearly seen in Fig. 13. They include the maximum damping, minimum damping, bifurcation points and points close to the load flow feasibility boundary. Some of the obtained characteristic points are summarized in Table 2.

TABLE 2
LOAD POWERS AT SOME CHARACTERISTIC SMALL SIGNAL STABILITY POINTS

| Bus | 1st minimum damping point | | 2nd minimum damping point | | Bifurcation point | |
|---|---|---|---|---|---|---|
| | $P_{ld}$ | $Q_{ld}$ | $P_{ld}$ | $Q_{ld}$ | $P_{ld}$ | $Q_{ld}$ |
| 1 | 0 | 0 | 0 | 0 | 0 | 0 |
| 2 | 0 | 0 | 0 | 0 | 0 | 0 |
| 3 | 0 | 0 | 0 | 0 | 0 | 0 |
| 4 | 0.0000 | -0.0000 | 0.0000 | -0.0000 | 0.0000 | -0.0000 |
| 5 | -0.8125 | -0.3250 | -0.5000 | -0.2000 | -0.5781 | -0.2313 |
| 6 | -0.5850 | -0.1950 | -0.3600 | -0.1200 | -0.4163 | -0.1388 |
| 7 | 0.0000 | -0.0000 | 0.0000 | -0.0000 | 0.0000 | -0.0000 |
| 8 | -0.6500 | -0.2275 | -0.4000 | -0.1400 | -0.4625 | -0.1619 |
| 9 | 0.0000 | 0.0000 | 0.0000 | 0.0000 | 0.0000 | -0.0000 |

In the examination of the proposed method based on the optimization problem (10) –(15), the method has been applied to locate these points of interest. The results showed that the constrained optimization procedure converged toward all the points of interests depending the initial guess of variables. The initial guesses were chosen using the routh estimates of the characteristic points obtained in preliminary examination.

## IV. Conclusion

A new method which computes the minimum and maximal damping, saddle node and Hopf bifurcations and load flow feasibility boundary points as part of a common procedure has been developed in the paper. The method has been tested and validated by numerical simulations, comparison with the previous results obtained for the used test systems, and by transient simulations conducted at the characteristic points. Further work is required to develop techniques for obtaining the initial guesses of variables, fast and reliable solving the constrained optimization problem, and handling of large power systems. Various practical applications of the new method await for further developments as well.

## V. Acknowledgement

This work was sponsored in part by an Australian Electricity Supply Industry Research Board grant "Voltage Collapse Analysis and Control".

Z. Y. Dong's research work was supported by Sydney University Electrical Engineering Postgraduate Scholarship.

## References

[1] V. Ajjarapu and B. Lee, "Bibliography on Voltage Stability," Iowa State University, see WWW site *http://www.ee.iastate.edu/ venkatar/VoltageStabilityBib*.

[2] I. Dobson, "Computing a Closest Bifurcation in Stability Multidimensional Parameter Space", *Journal of Nonlinear Science*, Vol. 3., No. 3., pp.307–327, 1993.

[3] Y. V. Makarov, D. J. Hill and J. V. Milanovic, "Effect of Load Uncertainty on Small Disturbance Stability Margins in Open-Access Power Systems", *Proc. Hawaii International Conference on System Sciences HICSS-30*, Kihei, Maui, Hawaii, January 7-10, 1997, Vol. 5, pp. 648–657.

[4] P. W. Sauer, B. C. Lesieutre and M. A. Pai, "Maximum Loadability and Voltage Stability in Power Systems," *International Jour-*

*nal of Electrical Power and Energy Systems*, Vol. 15, pp. 145–154, June 1993.

[5] M. A. Pai "Structural Stability in Power Systems," J. H.Chow, P. V. Kokotovic and R. J. Thomas edit, in *Systems and Control Theory for Power Systems*, Springer-Verlag, 1995, pp. 259–281.

[6] P. W. Sauer and B. C. Lesieutre, "Power System Load Modeling," J. H.Chow, P. V. Kokotovic and R. J. Thomas edit, in *Systems and Control Theory for Power Systems*, Springer-Verlag, 1995, pp. 283–313.

[7] P. W. Sauer and M. A. Pai, "Power System Steady-state Stability and the Load-Flow Jacobian", *IEEE Trans. on Power Systems*, Vol. 5, No. 4, November 1990, pp. 1374–1383.

[8] M. A. Pai, A. Kulkarni and P. W. Sauer, "Parallel Dynamic Simulation of Power Systems", *IEEE CH2868-8/90/0000*, pp. 1264–1267.

[9] C. Gajagopalan, B. Leisieutre, P. W. Sauer and M. A. Pai, "Dynamic Aspects of Voltage/Power Characteristics", *IEEE/PES 91 SM 419-2 PWRS.*

[10] C. Rajagopalan, P. W. Sauer and M. A. Pai, "Analysis of Voltage Control Systems Exhibiting Hopf Bifurcation", *Proceedings of the 28th Conference on Decision and Control*, Tampa, Florida, December 1989, pp. 332–335.

[11] C. Rajagopalan, P. W. Sauer and M. A. Pai, "An Integrated Approach to Dynamic and Static Voltage Stability", *ACC'89* Pittsburgh, June 21-23, 1989.

[12] B. Lee and V. Ajjarapu, "Bifurcation Flow: A Tool to Study Both Static and Dynamic Aspects of Voltage Stability", *Proceedings of the Bulk Power System Voltage Phenomena III. Voltage Stability, Security and Control*, Davos, Switzerland, Aug. 22-26, 1994, pp. 305–324.

[13] H. G. Kwatny, R. F. Fischl and C. Nwankpa, "Local Bifurcation in Power Systems: Theory, Computation and Application", D. J. Hill (ed), *Special Issue on Nonlinear Phenomena in Power Systems: Theory and Practical Implications, IEEE Proceedings,* Vol. 83, No. 11, November, 1995, pp. 1456–1483.

[14] V. Venkatasubramanian, H. Schättler and J. Zaborszky, "Dynamics of Large Constrained Nonlinear Systems -A Taxonomy Theory", D. J. Hill (ed), *Special Issue on Nonlinear Phenomena in Power Systems: Theory and Practical Implications, IEEE Proceedings,* Vol. 83, No. 11, November, 1995, pp. 1530–1561.

[15] V.A. Venikov, V.A. Stroev, V.I. Idelchik and V.I. Tarasov, "Estimation of Electric Power System Steady-State Stability in Load Flow Calculation," *IEEE Trans. on Power Apparatus and Systems*, Vol. PAS-94, May-June 1975, pp. 1034-1041.

[16] P. W. Sauer and M. A. Pai, "Power System Steady-State Stability and the Load-Flow Jacobian", *IEEE Trans. on Power Systems*, Vol. 5, No. 4, November 1990, pp. 1374–1383.

[17] Z. Y. Dong, Y. V. Makarov and D. J. Hill, "Computing the Aperiodic and Oscillatory Small Signal Stability Boundaries in the Modern Power Grids", *Proc. Hawaii International Conference on System Sciences HICSS-30*, Kihei, Maui, Hawaii, January 7-10, 1997.

[18] Y. V. Makarov, V. A. Maslennikov and D. J. Hill, "Calculation of Oscillatory Stability Margins in the Space of Power System Controlled Parameters", *Proc. of the International Symposium on Electric Power Engineering Stockholm Power Tech: Power Systems*, Stockholm, Sweden, 18-22 June, 1995, pp. 416-422

[19] Y. V. Makarov and I. A. Hiskens, "A Continuation Method Approach to Finding the Closest Saddle Node Bifurcation Point", *Proc. NSF/ECC Workshop on Bulk Power System Voltage Phenomena III*, Davos, Switzerland, August 1994.

[20] I. A. Hiskens and R. J. Davy, "A Technique for Exploring the Power Flow Solution Space Boundary", *Proc. of the International Symposium on Electric Power Engineering Stockholm Power Tech*, Vol. Power Systems, Stockholm, Sweden, June 1995, pp. 478-483.

[21] P. Kundur, *Power System Stability and Control*, New York: McGraw-Hill, 1994.

[22] D. J. Hill, V. A. Maslennikov, S. M. Ustinov, Y. V. Makarov, A. Manglick, B. Elliott, N. Rotenko and D. Conroy, "Advanced Small Disturbance Stability Analysis Techniques and MATLAB Algorithms" A final Report of the work *"Collaborative Research Project Advanced System Analysis Techniques" with the New South Wales Electricity Transmission Authority and The Department of Electrical Engineering, The University of Sydney"*, April 1996.

[23] I. A. Gruzdev, V. A. Maslennikov and S. M. Ustinov, "Development of Methods and Software for Analysis of Steady-State Stability and Damping of Bulk Power Systems," *In: Methods and Software for Power System Oscillatory Stability Computations*, Publishing House of the Federation of Power and Electro-Technical Societies, St. Petersburg, Russia, 1992, pp. 66-88 (in Russian).

[24] Y.V. Makarov, A.M. Kontorovich, D. J. Hill and I. A. Hiskens, "Solution Characteristics of Quadratic Power Flow Problems", *Proc. 12-th Power System Computation Conference,* Vol. 1, Dresden, Germany, 19-23 August, 1996, pp. 460-467.

[25] H. -D. Chiang, I. Dobson, et al. "On Voltage Collapse in Electric Power Systems," *IEEE Trans. Power Systems,* Vol. 5, No. 2, May 1990.

[26] P. M. Anderson and A. A. Fouad, *Power System Control and Stability*, Iowa State University Press, Ames, IA. 1977.

[27] J. H. Chow, editor, *Time-Scale Modeling of Dynamic Networks with Applications to Power Systems,* Springer-Verlag, Berlin, 1982.

[28] J. H. Chow and K. W. Cheung, "A Toolbox for Power System Dynamics and Control Engineering Education and Research", *IEEE/PES Trans. on Power Systems*, Vol. 7, No. 4, November 1992.

[29] H. G. Kwatny, X. -M. Yu and C. Nwankpa, "Local Bifurcation Analysis of Power Systems Using MATLAB", *95CH35764, Proceedings of the 4th IEEE Conference on Control Applications,* Albany, N. Y. September 28-29, 1995, pp. 57–62.

[30] M. K. Pal, "Voltage Stability Analysis Needs, Modeling Requirement, and Modeling Adequacy," *IEE Proceedings of Part C.*, Vol. 140, pp. 279–286, July 1993.

[31] A. Grace, "Optimization TOOLBOX User's Guide," The MathWorks, Inc. October 1994.

[32] J. H. Chow and A. Gebreselassie, "Dynamic Voltage Stability Analysis of a Single Machine Constant Power Load System", *Proc. 29th Conference on Decision and Control*, Honolulu Hawaii, December 1990, pp. 3057–3062.

[33] . P.E. Gill, W. Murray and M. H. Wright, *Practical Optimization*, Academic Press, 1981.

**Yuri V. Makarov** received the Ph.D. in Electrical Networks and Systems (1984) from the St. Petersburg State Technical University (former Leningrad Polytechnic Institute), Russia. He is an Associate Professor at Department of Power Systems and Networks in the same University. Now he is conducting his research work occupying a senior research position at the Department of Electrical Engineering in the University of Sydney, Australia. His research interests are mainly in the field of power system analysis, stability and control.

**Zhao Yang Dong** was born in China, 1971. He received his BSEE degree as first class honor in July, 1993. Since 1994, he had been studying in Tianjin University (Peiyang University), Tianjin, China for his MSEE degree. Now, he is continuing his study as a postgraduate research student in the Department of Electrical Engineering, the University of Sydney, Australia. His research interests include power system analysis and control, electric machine and drive systems areas.

**David J. Hill** (M'76, SM'91, F'93) received his B.E. and B.Sc. degrees from the University of Queensland, Australia in 1972 and 1974 respectively. In 1976 he received his Ph.D. degree in Electrical Engineering from the University of Newcastle, Australia. He currently occupies the Chair in Electrical Engineering at the University of Sydney. He is also a Head of Electrical Engineering Department at the same University. Previous appointments include research positions at the University of California, Berkeley and the Department of Automatic Control, Lund Institute of Technology, Sweden. From 1982 to 1993 he held various academic positions at the University of Newcastle. His research interests are mainly in nonlinear systems and control, stability theory, power system dynamics and security. His resent applied work consists of various projects in power system stabilization and power plant control carried out in collaboration with utilities in Australia and Sweden.